Modeling Hepatitis B Virus X–Induced Hepatocellular Carcinoma in Mice With the Sleeping Beauty Transposon System

Vincent W. Keng,[1,2,3] Barbara R. Tschida,[1,2] Jason B. Bell,[1,2] and David A. Largaespada[1,2,3,4]

The mechanisms associated with hepatitis B virus (HBV)–induced hepatocellular carcinoma (HCC) remain elusive, and there are currently no well-established animal models for studying this disease. Using the Sleeping Beauty transposon as a delivery system, we introduced an oncogenic component of HBV, the hepatitis B virus X (*HBx*) gene, into the livers of fumarylacetoacetate hydrolase (*Fah*) mutant mice via hydrodynamic tail vein injections. Coexpression of *Fah* complementary DNA from the transposon vector allowed for the selective repopulation of genetically corrected hepatocytes in *Fah* mutant mice. The process of hydrodynamic delivery induced liver inflammation, and the subsequent selective repopulation of hepatocytes carrying the transgene(s) could provide useful genetic information about the mechanisms of HBV-induced hyperplasia. Short hairpin RNA directed against transformation-related protein 53 (*shp53*) or other tumor suppressor genes and oncogenes [e.g., constitutively active neuroblastoma RAS viral (v-ras) oncogene homolog with Gly12Val substitution ($NRAS^{G12V}$)] could also be codelivered with *HBx* by this system so that we could determine whether oncogenic cooperation existed. We found that the expression of *HBx* induced the activation of β-catenin expression in hydrodynamically injected livers, and this indicated its association with the *Wnt* signaling pathway in HBV-induced hyperplasia. *HBx* coinjected with *shp53* accelerated the formation of liver hyperplasia in these mice. As expected, constitutively active $NRAS^{G12V}$ alone was sufficient to induce liver hyperplasia, and its tumorigenicity was augmented when it was coinjected with *shp53*. Interestingly, *HBx* did not seem to cooperate with constitutively active $NRAS^{G12V}$ in driving liver tumorigenesis. *Conclusion:* This system can be used as a model for studying the various genetic contributions of HBV to liver hyperplasia and finally HCC in an *in vivo* system. (HEPATOLOGY 2010;000:000-000.)

The activation of proto-oncogenes and the loss of tumor suppressor genes generated by epigenetic and genetic mechanisms have been implicated in the tumorigenesis of hepatocellular carcinoma (HCC). Presently, there is no consensus on the number of different HCC molecular subtypes, although a recent meta-analysis based on gene expression and genetic changes has suggested three main subtypes.[1] Hepatitis B virus (HBV) infection appears to play multiple roles in hepatocellular carcinogenesis.[2] The study of HBV pathogenesis has been difficult because there currently is no good animal model that combines hepatocyte necrosis and repopulation along with facile viral gene delivery (GD).

The unique regulatory component gene X of HBV encodes a 17-kDa protein called hepatitis B virus X (HBx; 154 amino acid residues). The *HBx* gene has been shown to induce cell proliferation and proapoptotic and stress responses, activate certain signal transduction

Abbreviations: Ab, antibody; ACTB, β-actin; AFP, alpha-fetoprotein; AKT, v-akt murine thymoma viral oncogene homolog 1; ALT, alanine aminotransferase; CTNNB1, β-catenin; FAH, fumarylacetoacetate hydrolase; FVB, inbred mouse strain FVB/N; GD, gene delivery; GFP, green fluorescent protein; HBV, hepatitis B virus; HBx, hepatitis B virus X; HCC, hepatocellular carcinoma; HE, hematoxylin-eosin; IHC, immunohistochemistry; $NRAS^{G12V}$, neuroblastoma RAS viral (v-ras) oncogene homolog with Gly12Val substitution; pAKT, phosphorylated v-akt murine thymoma viral oncogene homolog 1; PHI, post–hydrodynamic injection; PI3K, phosphoinositide 3-kinase; RT-PCR, reverse-transcription polymerase chain reaction; SB, Sleeping Beauty; shp53, short hairpin RNA directed against transformation-related protein 53; STAT3, signal transducer and activator of transcription 3; TP53, tumor protein p53.

From the [1]Masonic Cancer Center, [2]Center for Genome Engineering, [3]Department of Genetics, Cell Biology, and Development, and [4]Department of Pediatrics, University of Minnesota, Minneapolis, MN.

Received August 24, 2010; accepted November 11, 2010.

Vincent W. Keng, Barbara R. Tschida, and David A. Largaespada are supported by grant R01 CA132962 from the National Cancer Institute. Jason B. Bell is supported by grant R01 DK082516 from the National Institutes of Health.

J_ID: ZHE Customer A_ID: 10-1439.R1 Customer Art: ZHE24091 Date: 16-December-10 Stage: Page: 2

pathways and DNA repair mechanisms, and induce transformation.[3] *HBx* as a transgene in mice has produced variable effects.[4-6] It remains unclear whether and how *HBx* can induce HCC in transgenic mice.

The oncogenic mechanisms of *HBx* are also controversial. *HBx* has been variably reported to activate signal transducer and activator of transcription 3 (*STAT3*) and *WNT*/β-catenin (*CTNNB1*) or bind to and inactivate tumor protein p53 (TP53).[7-11] The critical activators of HBx in HCC induction have been difficult to identify because no efficient and rapid system for *in vivo* GD and oncogenesis has been available. In order to elucidate the effect of *HBx in vivo*, we used the Sleeping Beauty (*SB*) transposon system to deliver this transgene stably via hydrodynamic tail vein injections into the livers of fumarylacetoacetate hydrolase (*Fah*)–deficient mice.[12] Because mutations in *TP53* are common in patients with HBV-induced HCC, we cointroduced a transposon containing short hairpin RNA directed against transformation-related protein 53 (*shp53*) to study this relationship. Also, to elucidate whether any relationship exists between *HBx* infection and neuroblastoma RAS viral (v-ras) oncogene homolog (*NRAS*) mutations, a transposon containing a constitutively active neuroblastoma RAS viral (v-ras) oncogene homolog with Gly12Val substitution ($NRAS^{G12V}$) was also cointroduced with *HBx*. Using this model, we were able to mimic *HBx* expression after HBV infection and then the subsequent repopulation of HBV-infected hepatocytes in the liver.

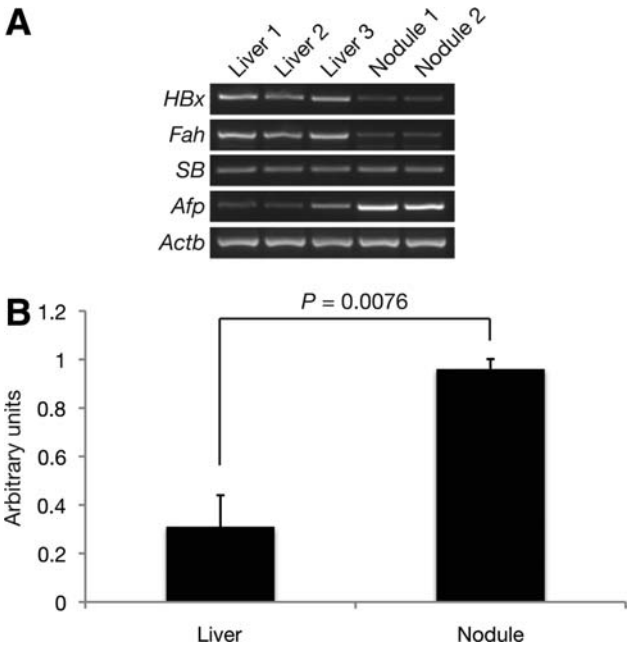

Fig. 1. Proliferative and oncogenic potential of *HBx* in a selectively repopulating liver. (A) RT-PCR analyses of liver nodules and adjacent normal livers at 139 days PHI expressed *HBx* and *Fah* transgenes. (B) An RT-PCR semiquantitative analysis demonstrated significantly higher *Afp* expression in the aforementioned hyperplastic nodules versus the adjacent normal livers ($P = 0.0076$, unpaired *t* test) with respect to *Actb* levels.

Materials and Methods

Generation of Fah-Deficient/Rosa26-SB11 Mice. All animal work was conducted according to an institutionally approved animal welfare protocol. The generation, maintenance, and genotyping of doubly transgenic mice ($Fah^{-/-}$ *Rosa26*-SB11)[13,14] are described in the Supporting Methods.

Generation of Transgenes Used for Hydrodynamic Tail Vein Injections. We generated pKT2/GD plasmids carrying *HBx*, $NRAS^{G12V}$, green fluorescent protein (*Gfp*), an empty vector, or a transposon vector containing *shp53* (pKT2/GD-HBx, pKT2/GD-NRAS, pKT2/GD-Gfp, pKT2/GD-empty, and pT2/shp53, F1 respectively; Supporting Information Fig. 1A)[15] with standard molecular cloning techniques. The steps are described in detail in the Supporting Methods.

Hydrodynamic Tail Vein Injections. Twenty micrograms of each construct was hydrodynamically injected into 4- to 6-week-old, doubly transgenic male mice as described previously.[16] These mice were normally maintained on 2-(2-nitro-4-trifluoromethylbenzoyl)-1,3-cyclohexanedione drinking water, but this was replaced with normal drinking water immediately after the hydrodynamic injection of transposon vector(s).

Liver Analysis. Whole livers were removed and weighed, and the number of visible macroscopic hyperplastic nodules was counted. Reasonably sized nodules were carefully removed for DNA and RNA extraction. Histological sections were also taken from larger nodules for hematoxylin-eosin (HE) or immunohistochemistry (IHC) analyses as described in the Supporting Methods.

Address reprint requests to: David A. Largaespada, Ph.D., Masonic Cancer Center, University of Minnesota, 420 Delaware Street Southeast, Minneapolis, MN 55455. E-mail: larga002@umn.edu; fax: 612-626-6140.

View this article online at wileyonlinelibrary.com.
DOI 10.1002/hep.24091
Potential conflict of interest: Nothing to report.
Additional Supporting Information may be found in the online version of this article.

J_ID: ZHE Customer A_ID: 10-1439.R1 Customer Art: ZHE24091 Date: 16-December-10 Stage: Page: 3

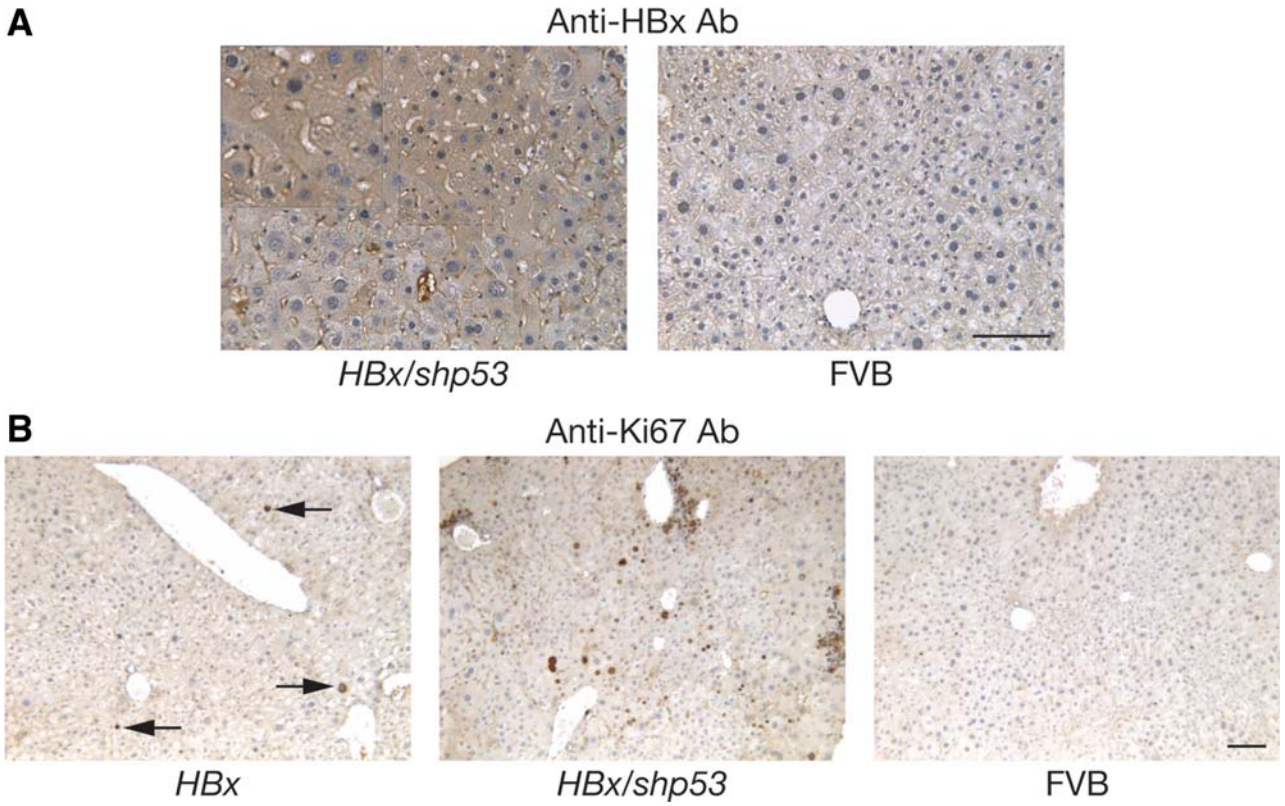

COLOR

Fig. 2. Augmented oncogenic potential of *HBx* with *shp53* in a selectively repopulating liver. (A) Representative demonstration of HBx-positive hepatocytes by IHC in a 71-day PHI *HBx*/*shp53* mouse (see also the magnified insert in the upper left corner of the dashed area). HBx was not detected in the normal FVB liver (scale bar = 100 μm). (B) Representative demonstration of a high mitotic index by Ki67 IHC in a 71-day PHI *HBx*/*shp53* mouse. A representative field of view containing several Ki67-positive cells (arrows) in a 78-day PHI *HBx* mouse is shown. Ki67 was not detected in the normal FVB liver (scale bar = 100 μm). Negative controls for panels A and B (serial sections incubated without the indicated primary Abs) gave no visible signals above the background (data not shown). Abbreviations: Ab, antibody; FVB, inbred mouse strain FVB/N.

Blood Serum Analyses. Alanine aminotransferase (ALT) levels in blood serum samples were analyzed by Marshfield Laboratories (Marshfield, WI).

Reverse-Transcription Polymerase Chain Reaction (RT-PCR). The protocol is described in detail in the Supporting Methods.

Results

Effect of the HBx Transgene During Selective Liver Repopulation. Mice injected with *HBx* alone (Supporting Information Fig. 1A) were observed for up to 139 days post–hydrodynamic injection (PHI; n = 16). The detection of luciferase activity at 48 days PHI indicated selective repopulation of the liver as a result of stable transgene integration into the mouse genome mediated by *SB* transposition (Supporting Information Fig. 1B, top). The majority of *HBx* animal livers displayed no evidence of hyperplasia (88%). However, two *HBx* animals sacrificed at 74 and 139 days PHI displayed livers with hyperplastic nodules (Supporting Information Fig. 1C). Hyperplastic nodules isolated at 139 days PHI were positive for *HBx* transcripts by RT-PCR (Fig. 1A). These hyperplastic nodules expressed high levels of alpha-fetoprotein (*Afp*), a known diagnostic marker for HCC, in comparison with the adjacent normal liver (Fig. 1A). According to semiquantitative RT-PCR analyses, the arbitrary expression levels of *Afp* with respect to β-actin (*Actb*) were 0.31 $\pm$ 0.13 and 0.96 $\pm$ 0.042 (means and standard deviations) in normal livers and hyperplastic nodules, respectively (P = 0.0076; Fig. 1B). In order to visualize the selective hepatocyte repopulation process, control mice injected with *Gfp* alone (Supporting Information Fig. 1A) were observed for up to 113 days PHI (n = 4). The detection of luciferase activity at 48 days PHI also indicated selective repopulation of the liver (Supporting Information Fig. 1B, bottom). These *Gfp* mice were sacrificed at 82 and 113 days PHI (n = 4). Although no hyperplastic nodules were initially detected at 82 days PHI (n = 2), a single *Gfp*-negative nodule was detected at 113 days PHI (n = 2). Viewed with fluorescent imaging, the *Gfp* expression pattern confirmed that the liver

ID: srinivasanv | Black Lining: [ON] | Time: 17:04 | Path: N:/Wiley/3b2/HEP#/Vol00000/100611/APPFile/JW-HEP#100611

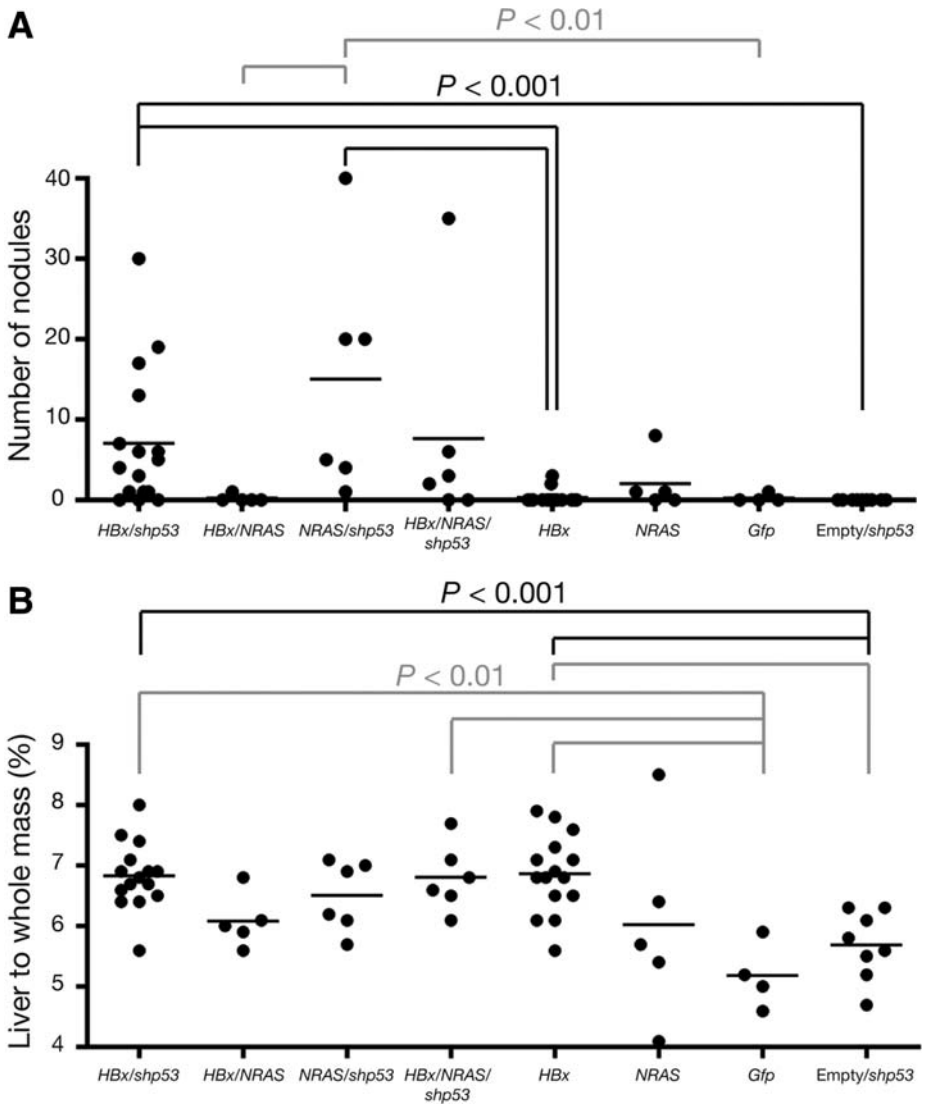

Fig. 3. *NRAS* does not cooperate with *HBx* in liver tumorigenesis during selective repopulation. (A) A statistical analysis using the two-tailed Mann-Whitney test indicated a highly significant difference ($P < 0.001$, black lines) in the number of nodules between the indicated cohorts. Significant differences ($P < 0.01$, gray lines) were seen between the indicated cohorts. Marginal significance ($P < 0.05$) in the number of nodules was seen between *HBx*/*shp53* and *HBx*/*NRAS*, between *HBx*/*shp53* and *Gfp*, between *HBx* and *HBx*/*NRAS*/*shp53*, and between empty/*shp53* and *HBx*/*NRAS*/*shp53* (not indicated). (B) A statistical analysis using the two-tailed test Mann-Whitney indicated a highly significance difference ($P < 0.001$, black lines) in the liver weight percentage with respect to the whole mouse mass in each injected cohort. A statistical analysis using the two-tailed Mann-Whitney test indicated a significance difference ($P < 0.01$, gray lines) in the liver weight percentage between the indicated cohorts. Marginal significance ($P < 0.05$) in the liver weight percentage was seen between *HBx*/*shp53* and *HBx*/*NRAS*, between *HBx* and *HBx*/*NRAS*, between empty/*shp53* and *NRAS*/*shp53*, between *NRAS*/*shp53* and *Gfp*, and between *HBx*/*shp53* and *Gfp* (not indicated).

repopulation process occurred uniformly (Supporting Information Fig. 1D). Importantly, control mice coinjected with an empty vector and *shp53* (empty/*shp53*; Supporting Information Fig. 1A) were negative for hyperplasia up to 139 days (n = 9). Interestingly, Ki67 staining did not show a significant increase in the mitotic index for *Gfp* animals (data not shown). However, there were higher levels of Ki67 staining in *HBx* animals (Fig. 2B). The liver weight percentage of *HBx* mice was significantly higher than that of *Gfp* mice ($P < 0.01$) and empty/*shp53* controls ($P < 0.001$; Fig. 3B), and this indicates that *HBx* may have a proliferative effect on hepatocytes. Mice injected with *HBx* alone had high levels of *Ctnnb1* expression by IHC, and this was mainly localized in the cellular membrane of repopulated hepatocytes (Fig. 4). Livers of *HBx* mice had hardly detectable levels of phosphorylated v-akt murine thymoma viral oncogene homolog 1 (pAkt; Fig. 5) and displayed more CD45 staining cells by IHC in comparison with control *Gfp* animals (Supporting Information Fig. 4). Interestingly, ALT levels among *HBx*, empty/*shp53*, and *Gfp* representative animals were not significantly different (Table 1).

Synergistic Effects of HBx and shp53 Transgenes for Tumorigenesis During Selective Liver Repopulation. Mice injected with *HBx* and *shp53* (*HBx*/*shp53*; Supporting Information Fig. 1A) were observed for up to 139 days PHI (n = 16). *HBx*/*shp53* animals were sacrificed at various time points between 63 and 139 days PHI. Although no hyperplastic nodules were initially detected at 63 days PHI, the *HBx*/*shp53* mouse liver had a rough surface texture (Supporting Information Fig. 2A, middle), and this indicated possible hyperproliferation and/or hyperplasia. The roughly textured liver was also *Gfp*-positive (detection of the *Gfp* reporter gene within *shp53*) and nodular in appearance when it was viewed under a fluorescent microscope (Supporting Information Fig. 2B, middle). Empty/*shp53* mice were sacrificed at various time points

J_ID: ZHE Customer A_ID: 10-1439.R1 Customer Art: ZHE24091 Date: 16-December-10 Stage: Page: 5

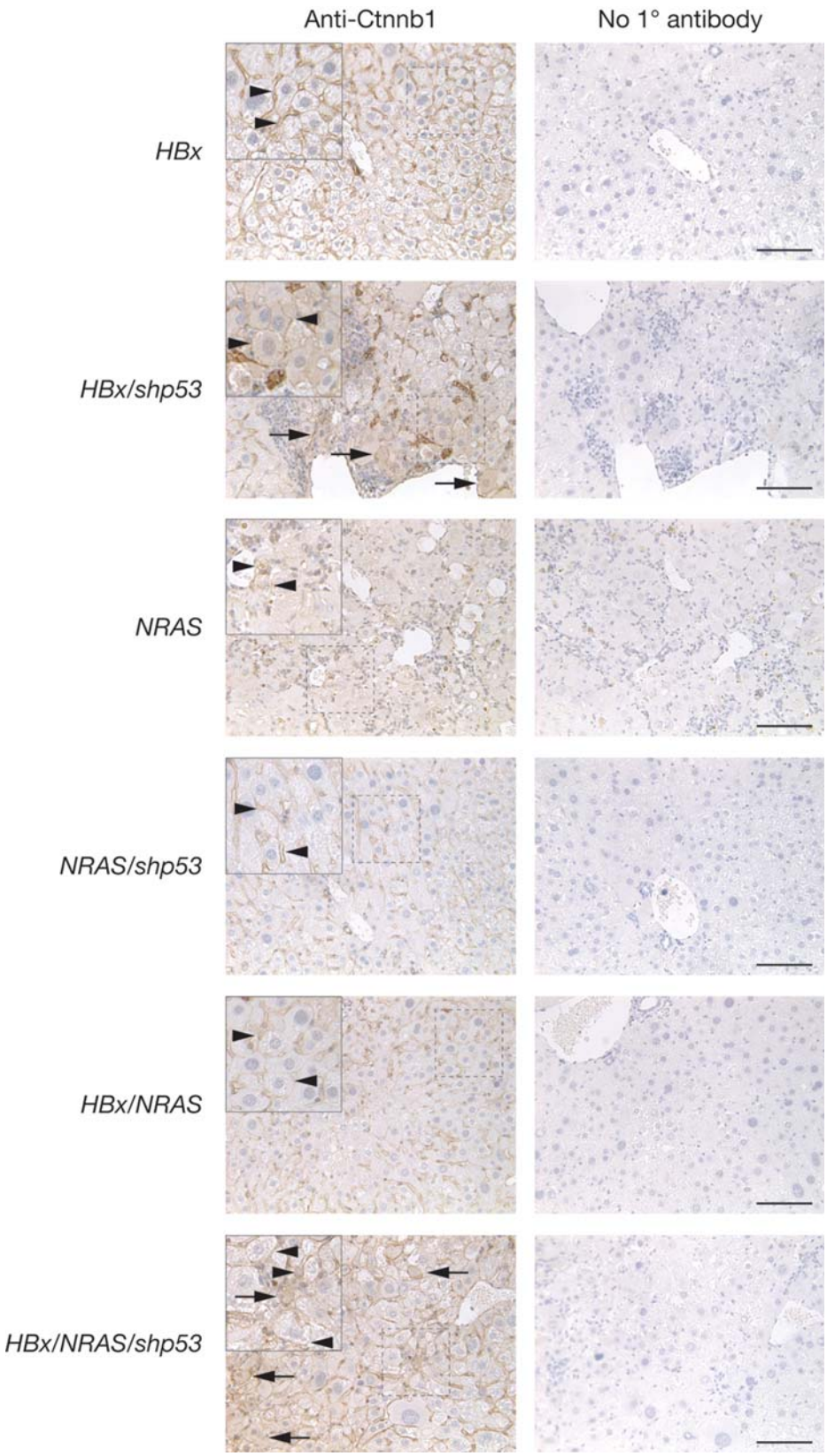

COLOR

Fig. 4. The oncogenic potential of *HBx* is associated with the *Wnt* signaling pathway. IHC staining is shown for serial liver sections taken from experimental animals injected with the indicated transgene(s) with an antibody against Ctnnb1: a 78-day PHI experimental animal injected with *HBx* alone (*HBx*), a 72-day PHI experimental animal injected with *HBx* and *shp53* (*HBx*/*shp53*), an 82-day PHI experimental animal injected with *NRAS* alone (*NRAS*), a 71-day PHI experimental animal injected with *NRAS* and *shp53* (*NRAS*/*shp53*), a 71-day PHI experimental animal injected with *HBx* and *NRAS* (*HBx*/*NRAS*), and a 71-day PHI experimental animal injected with *HBx*, *NRAS*, and *shp53* (*HBx*/*NRAS*/*shp53*). The left column shows sections incubated with anti-Ctnnb1; the right column shows sections with no primary antibody. Magnified inserts in the upper left corners are indicated by dashes. Arrows and arrowheads indicate Ctnnb1 cytoplasmic and membranous staining, respectively, detected in indicated cells (scale bar = 100 μm).

between 63 and 139 days PHI (n = 9). No hyperplasia was seen in the liver of the empty/*shp53* mouse at 63 days PHI (Supporting Information Fig. 2A, left), and uniform *Gfp* expression was detected throughout the liver (Supporting Information Fig. 2B, left). In contrast, 86% of *HBx*/*shp53* mice (n = 7) sacrificed at

ID: srinivasanv | Black Lining: [ON] | Time: 17:04 | Path: N:/Wiley/3b2/HEP#/Vol00000/100611/APPFile/JW-HEP#100611

J_ID: ZHE Customer A_ID: 10-1439.R1 Customer Art: ZHE24091 Date: 16-December-10 Stage: Page: 6

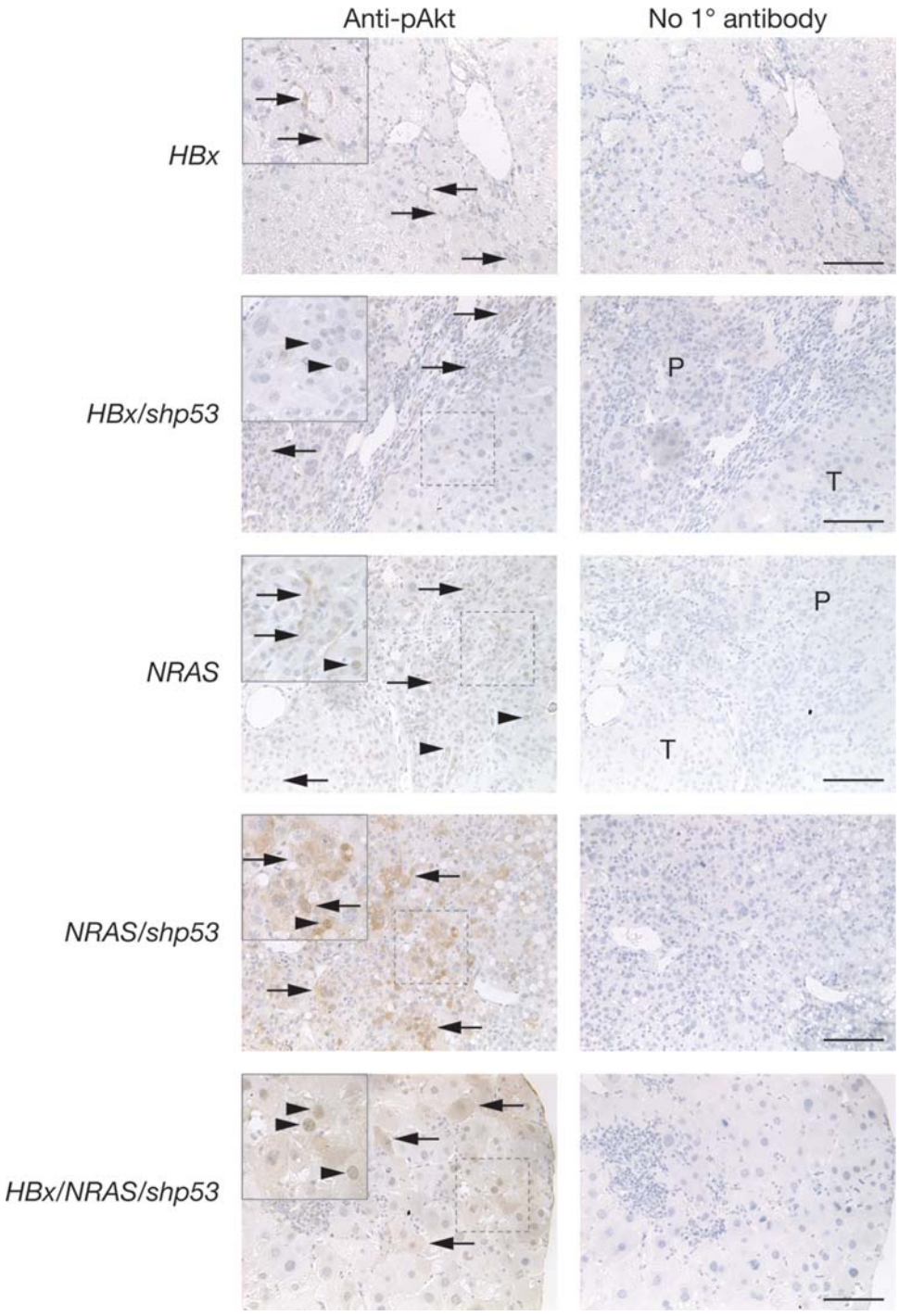

COLOR

Fig. 5. The oncogenic potential of *NRAS* is associated with the *Pi3k/Akt* signaling pathway. IHC staining is shown for serial liver sections taken from experimental animals injected with the indicated transgene(s) with an antibody against pAkt (see Fig. 4 for descriptions of the *HBx*, *HBx/shp53*, *NRAS*, *NRAS/shp53*, and *HBx/NRAS/shp53* mice). The left column shows sections incubated with anti-pAkt; the right column shows sections with no primary antibody. Magnified inserts in the upper left corners are indicated by dashes. Arrows and arrowheads indicate pAkt cytoplasmic and nuclear staining, respectively, detected in indicated cells; P indicates parenchymal; and T indicates hyperplastic nodule (scale bar = 100 μm).

approximately 70 days PHI had multiple hyperplastic nodules (Supporting Information Fig. 2A, right) that were *Gfp*-positive (Supporting Information Fig. 2B, right). Livers of empty/*shp53* mice observed at various time points were normal, and the *Gfp* expression throughout the livers was relatively uniform (data not shown). The majority of hyperplastic nodules isolated from *HBx*/*shp53* animals at 72 days PHI were *Gfp*-positive, and the presence of *HBx* and/or *shp53* was confirmed by both RT-PCR (Supporting Information Fig. 2C) and IHC (Fig. 2A). Semiquantitative RT-PCR analysis demonstrated no statistical differences in *Afp* expression levels between hyperplastic nodules and adjacent normal livers isolated from 72-day PHI *HBx*/*shp53* animals (Supporting Information Fig. 2D). However, significant differences in *Afp* expression levels

ID: srinivasanv | Black Lining: [ON] | Time: 17:05 | Path: N:/Wiley/3b2/HEP#/Vol00000/100611/APPFile/JW-HEP#100611

Table 1. ALT Serum Levels in Representative Experimental Animals Injected With Various Transgenes

Injected Transgene(s)*	Number of Tested Animals	PHI (Days)	ALT in Blood Serum (U/L)†	Nodules/Appearance‡
Gfp	4	82 and 113	61.3 ± 22.3	Normal to 1 nodule
Empty/*shp53*	5	70 to 131	87.0 ± 28.3	Normal
HBx	9	71 to 78	79.7 ± 29.5	Rough to 3 nodules
HBx/*shp53*	9	71 to 74	146.8 ± 83.2	Rough to 30 nodules
HBx/*NRAS*	5	71 and 72	43.2 ± 25.5	Slightly rough to 1 nodule
HBx/*NRAS*/*shp53*	6	61 to 72	157 ± 110.9	Normal to 35 nodules
NRAS	5	82	57.6 ± 42.2	Normal to 8 nodules
NRAS/*shp53*	6	61 and 71	89.7 ± 19.0	1 to 40 nodules

*Gfp, pKT2/GD-Gfp; empty/*shp53*, pKT2/GD-empty and pT2/shp53; *HBx*, pKT2/GD-HBx; *HBx*/*shp53*, pKT2/GD-HBx and pT2/shp53; *HBx*/*NRAS*, pKT2/GD-HBx and pKT2/GD-NRAS; *HBx*/*NRAS*/*shp53*, pKT2/GD-HBx, pKT2/GD-NRAS, and pT2/shp53; *NRAS*, pKT2/GD-NRAS; and *NRAS*/*shp53*, pKT2/GD-NRAS and pT2/shp53.

†The data are presented as means and standard deviations.

‡*Normal* indicates no abnormalities; *slightly rough* indicates that the liver texture was slightly rough in appearance; *rough* indicates that the liver texture was rough in appearance; and *nodule* indicates hyperplastic liver nodule detection.

were seen between (1) empty/*shp53* and *HBx*/*shp53* normal livers ($P = 0.0035$) and (2) normal empty/*shp53* livers and *HBx*/*shp53* nodules ($P < 0.0001$; Supporting Information Fig. 2D). HBx was detected in *HBx*/*shp53* livers (Fig. 2A), and these animals generally had higher levels of Ki67 by IHC in comparison with animals injected with *HBx* alone (Fig. 2B). Although *HBx* alone was capable of inducing hyperplasia at low penetrance (74 days PHI) or after prolonged latency (139 days PHI), its oncogenic potential was augmented, as shown by reduced latency to 71 days PHI and greater tumor multiplicity, with the coinjection of the *shp53* transgene. *HBx*/*shp53* mice had levels of Ctnnb1 by IHC comparable to those of mice injected with *HBx* alone (Fig. 4). Expression of Ctnnb1 was mainly localized to the cellular membrane of *HBx* repopulated hepatocytes (Fig. 4). In addition to membranous Ctnnb1 staining, cytoplasmic staining was also detected in some hepatocytes of *HBx*/*shp53* animals (Fig. 4). Hyperplastic nodules taken from an *HBx*/*shp53* animal were weakly positive for pAkt (Fig. 5) and displayed more CD45 staining cells by IHC in comparison with *Gfp* animals (Supporting Information Fig. 4). ALT levels in representative *HBx*/*shp53* experimental animals were marginally significantly higher ($P < 0.05$) than those in *Gfp* or *HBx* animals, and they displayed a trend (not statistically significant) toward higher ALT levels in comparison with empty/*shp53* animals (Table 1).

HBx Does Not Cooperate With NRAS^{G12V} in Accelerating Liver Tumorigenesis During Selective Liver Repopulation. Hyperplasia was detected in 60% of mice injected with *NRAS*^{G12V} (*NRAS*, Supporting Information Fig. 1A) at 82 days PHI (n = 5; Supporting Information Fig. 3A, left). Histological analyses of these hyperplastic nodules by HE staining (Fig. 6A, left) and IHC confirmed the detection of *NRAS* in these nodules (Fig. 6B). This tumorigenic potential was augmented when mice were coinjected with *shp53* (*NRAS*/*shp53*), as shown by the accelerated detection of hyperplasia by 61 days PHI (n = 2). By 71 days PHI, hyperplasia was detected in all remaining *NRAS*/*shp53* mice (n = 4; Supporting Information Fig. 3A, middle). *NRAS*/*shp53* livers were *Gfp*-positive macroscopically (Supporting Information Fig. 3C, left) and were shown to express *Gfp* and *NRAS* by RT-PCR (Supporting Information Fig. 3D). Histological analyses of these hyperplastic nodules by HE staining (Fig. 6A, right) and IHC confirmed that *NRAS* and *shp53* contributed to the tumorigenesis (Fig. 6C). *NRAS*/*shp53* animals displayed a trend (not statistically significant) toward higher ALT levels in comparison with *NRAS* or *Gfp* animals (Table 1). *NRAS*/*shp53* livers displayed more CD45-positive staining cells than *Gfp* or *NRAS* (Supporting Information Fig. 4). In contrast, in mice coinjected with *HBx* and *NRAS* transgenes (*HBx*/*NRAS*; n = 5), only one hyperplastic nodule was isolated from a single experimental mouse at 70 days PHI (Supporting Information Fig. 3A, right). Besides this, the livers isolated from remaining *HBx*/*NRAS* mice were macroscopically normal in appearance (data not shown). Interestingly, *HBx*/*NRAS* livers displayed more CD45-positive staining cells than *Gfp* or *NRAS* livers (Supporting Information Fig. 4). ALT levels in *HBx*/*shp53* animals were significantly higher than those in *HBx*/*NRAS* animals ($P < 0.01$), and marginally significantly higher levels ($P < 0.05$) were seen in *HBx* and *NRAS*/*shp53* animals versus *HBx*/*NRAS* animals (Table 1). When all three transgenes were coinjected (*HBx*/*NRAS*/*shp53*), 67% of the mice (n = 6) sacrificed at 61 and 71 days PHI displayed multiple hyperplastic nodules (Supporting Information Fig. 3B). The majority of nodules were *Gfp*-positive (Supporting Information Fig. 3C, right) and were

J_ID: ZHE Customer A_ID: 10-1439.R1 Customer Art: ZHE24091 Date: 16-December-10 Stage: Page: 8

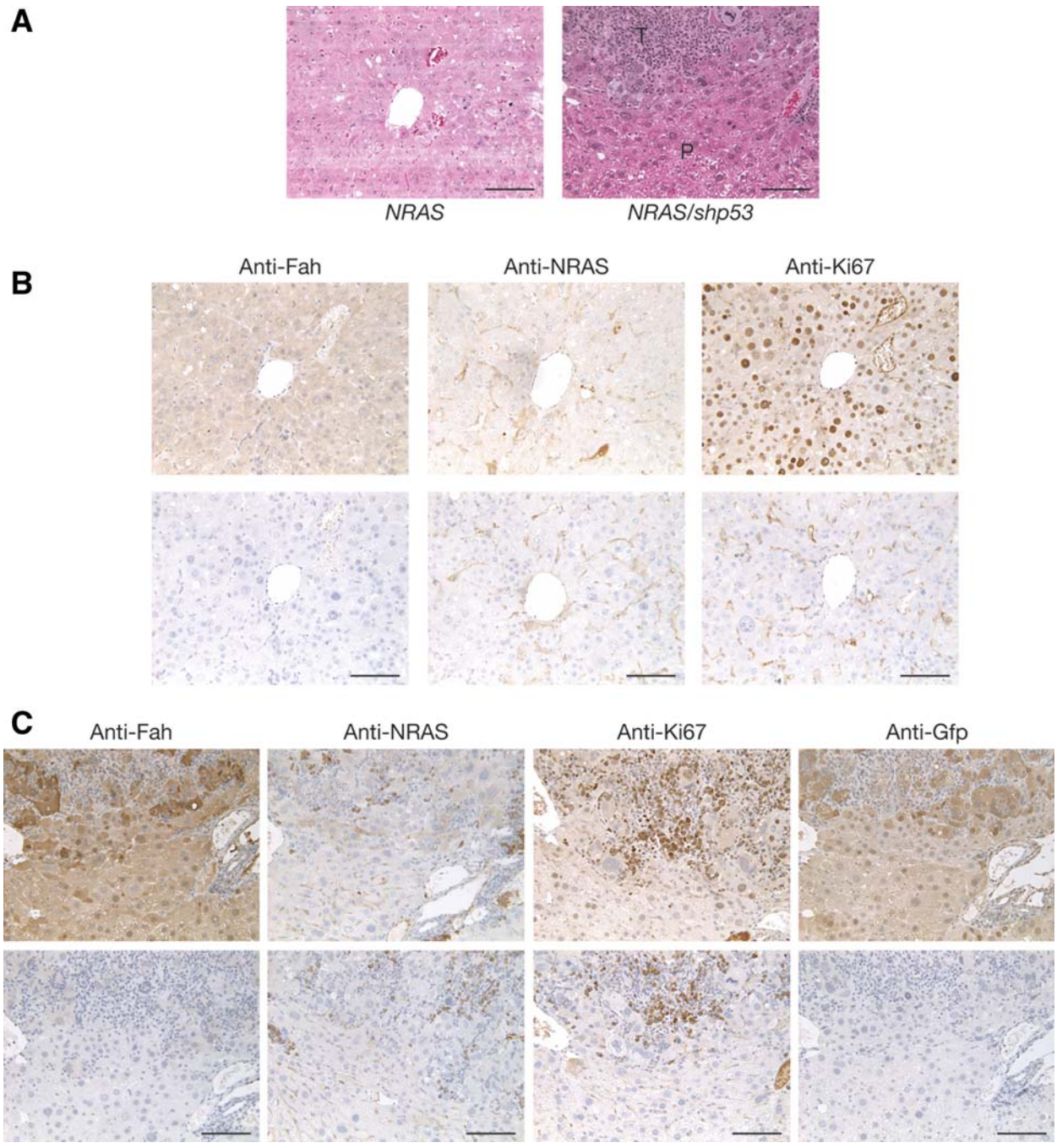

COLOR

Fig. 6. Oncogenic potential of *NRAS* alone or in combination with *shp53* in a selectively repopulating liver. (A) HE staining of hyperplastic nodule sections taken from experimental animals injected with *NRAS* alone at 82 days PHI or in combination with *shp53* at 71 days PHI. P indicates parenchymal, and T indicates hyperplastic nodule (scale bar = 100 μm). (B) IHC staining of hyperplastic nodule serial sections taken from experimental animals injected with *NRAS* alone at 82 days PHI with antibodies against Fah, NRAS, or Ki67. The top panels shows sections incubated with the indicated antibodies; the bottom panels show sections with no primary antibodies (scale bar = 100 μm). (C) IHC staining of hyperplastic nodule serial sections taken from *NRAS*/*shp53* experimental animals at 71 days PHI with antibodies against Fah, NRAS, Ki67, or Gfp (right). The top panels show sections incubated with the indicated antibodies; the bottom panels show sections with no primary antibodies (scale bar = 100 μm).

shown to express *Gfp* by RT-PCR (Supporting Information Fig. 3D). Expression of the injected transgenes was detected in the majority of normal livers and hyperplastic nodules isolated from both groups (*HBx*/*NRAS*/*shp53* and *NRAS*/*shp53*; Supporting Information Fig. 3D). ALT levels for *HBx*/*shp53* and *HBx*/*NRAS*/*shp53* animals were similar (Table 1). Semi-quantitative RT-PCR analyses also demonstrated a significant difference in the expression levels of *Afp* in hyperplastic nodules versus adjacent normal livers (*P*

ID: srinivasanv | Black Lining: [ON] | Time: 17:06 | Path: N:/Wiley/3b2/HEP#/Vol00000/100611/APPFile/JW-HEP#100611

= 0.0044, unpaired *t* test; data not shown). A statistical analysis using the two-tailed Mann-Whitney test indicated highly significant differences ($P < 0.001$) in the number of hyperplastic nodules between *HBx/shp53* and *HBx*, between *HBx/shp53* and empty/*shp53*, between *HBx* and *NRAS/shp53*, and between empty/*shp53* and *NRAS/shp53*. Significant differences ($P < 0.01$) were seen between *NRAS/shp53* and *HBx/NRAS* and between *NRAS/shp53* and *Gfp*. Marginal significance ($P < 0.05$) was seen between *HBx/shp53* and *HBx/NRAS*, between *HBx/shp53* and *Gfp*, between *HBx* and *HBx/NRAS/shp53*, and between empty/*shp53* and *HBx/NRAS/shp53* (Fig. 3A). A statistical analysis using the two-tailed Mann-Whitney test indicated highly significant differences ($P < 0.001$) in the weight percentage between *HBx/shp53* and empty/*shp53* and between *HBx* and empty/*shp53*. Significant differences ($P < 0.01$) were seen between *HBx/shp53* and *Gfp*, between *HBx* and *Gfp*, between empty/*shp53* and *HBx/NRAS/shp53*, and between *HBx/NRAS/shp53* and *Gfp*. Marginal significance ($P < 0.05$) was seen between *HBx/shp53* and *HBx/NRAS*, between *HBx* and *HBx/NRAS*, between empty/*shp53* and *NRAS/shp53*, between *NRAS/shp53* and *Gfp*, and between *HBx/shp53* and *Gfp* (Fig. 3B). Mice injected with *NRAS* alone generally had weak expression levels of Ctnnb1 detectable by IHC (Fig. 4). Hyperplastic nodules induced by *NRAS* coinjected with *shp53* generally had higher Ctnnb1 expression levels but not the levels seen in *HBx* or *HBx/shp53* mice (Fig. 4). As expected, *HBx/NRAS* mice had heterogeneous staining patterns for Ctnnb1 (Fig. 4). In contrast, hyperplastic nodules from *NRAS* or *NRAS/shp53* mice were highly positive for pAkt by IHC (Fig. 5).

Discussion

Using the *SB* transposon system and hydrodynamically introducing transgenes specifically into the livers of *Fah*-null/*SB* transposase–expressing recipient mice, we could dissect the contributions of various gene components of HBV by inducing liver hyperplasia in these animals. Our results demonstrate the oncogenic effect of the *HBx* transgene when it is hydrodynamically delivered into hepatocytes repopulating a liver. The low penetrance or delayed tumorigenic latency of *HBx* in injected mice may reflect the long latency of HBV-induced cirrhosis and tumorigenesis in infected humans. The fact that we observed an effect of *HBx* alone may indicate that its expression can cooperate with the process of hepatocyte regrowth to induce liver hyperplasia. Mice injected with *HBx* alone seem to have higher liver to whole mass percentages, and this indicates that *HBx* may have a hyperproliferative effect during HBV-induced liver tumorigenesis (Fig. 3B). Tumor latency was reduced and the oncogenic effect was augmented when *HBx* was coinjected with *shp53*. This is especially important because approximately 50% of human patients with HCC have mutations in the *TP53* gene. *HBx* has been shown to bind *TP53* and inactivate its activity,[9,11] but our data indicate that this mechanism must not impair *TP53* function sufficiently for tumor formation. Therefore, *TP53* mutant hepatocytes in a patient who acquires an HBV infection would likely lead to an enhanced risk of transformation to HCC.

Our results indicate that *HBx* does not seem to cooperate with constitutively active *NRAS* to induce liver tumorigenesis in *HBx/NRAS* animals. This was evident from the relatively low ALT levels in serum (Table 1), the low tumor multiplicity, and the liver weight to whole mass percentage (Fig. 3A,B) in *HBx/NRAS* mice. *HBx* has been suggested to up-regulate the *Ras* signaling pathway.[17] Perhaps *HBx* expression and activated *Ras* are redundant in this transformation assay. Even when all the transgenes were coinjected (*HBx/NRAS/shp53*), there was only a marginally significant increase ($P < 0.05$) in tumorigenicity in comparison with *HBx* alone. Moreover, no significant increase in tumorigenicity was seen in *HBx/NRAS* animals versus animals with *NRAS* alone (Fig. 3A). Our results indicate that *HBx* up-regulates the *Wnt* signaling pathway, and this may play a role in liver tumorigenesis (Fig. 4), whereas constitutively active *NRAS* seems to induce hyperplasia, probably via the *RAF*/mitogen-activated protein kinase kinase/extracellular signal-regulated kinase and/or phosphoinositide 3-kinase (*PI3K*)/v-akt murine thymoma viral oncogene homolog 1 (*AKT*) associated pathways (Fig. 5). In addition, we detected high levels of CD45-positive staining cells in livers of animals injected with *HBx* alone or in combination with other transgenes (Supporting Information Fig. 4). These cells could represent infiltrating lymphocytes, which are often associated with HBV infection. Indeed, the HBx protein would be predicted to act as a foreign antigen in our system, unlike previously reported *HBx* transgenic mouse models. HBx-induced inflammation may play some role in HCC progression; this hypothesis could be tested with our model. Elevated pAkt levels were detected by IHC in experimental animals injected with *NRAS* alone or in combination with *shp53*, and this indicates that *NRAS* is likely signaling via the *Pi3k/Akt* pathway (Fig. 5). *HBx* has been previously shown to activate the *WNT/*

CTNNB1 signaling pathway in human hepatoma cell lines.[8] *HBx* antigen has also been associated with the accumulation of *CTNNB1* in the cytoplasm and/or nucleus and the up-regulation of the *HBx* antigen effector up-regulated gene 11, which results in increased activation of *CTNNB1*.[18] The *CTNNB1* staining pattern can be correlated with the histopathological types of liver tumors.[19] The absence of nuclear staining and strong membranous staining with rare, weak cytoplasmic expression of Ctnnb1 suggested that the hyperplastic nodules induced by *HBx* or *HBx*/*shp53* were adenocarcinomas or poorly differentiated HCC (Fig. 4). We did not detect any activation of Stat3 in liver tumors expressing *HBx* by IHC in our experimental cohorts with a phospho-Stat3 (Tyr705)–specific antibody (data not shown) despite the previous suggestion that *HBx* activates *Stat3*.[7] Finally, it should be stated that there will be a subpopulation of *Fah*-null cells that can escape the selection process by activating the survival *Akt* pathway caused by hepatic stress.[20] These cells can evolve by acquiring additional mutations and result in hyperplastic nodules not associated with the injected transgenes. Examples of such background *Fah*-negative nodules were seen in *HBx*/*shp53* and *HBx*/*NRAS*/*shp53* mice (Supporting Information Figs. 2C and 3D, respectively). These nodules were negative for the injected transgenes by RT-PCR. Such background tumors occur only at a low rate and can be segregated from transgene-induced tumors by molecular and biochemical tests. Nevertheless, our experience shows that the *Fah*-deficient mouse model, in combination with the *SB* transposon system, is useful for *in vivo* functional validation of HBV genes in liver hyperplastic induction. Therefore, our present study reinforces the previous observations associated with HBV infection and validates the use of our mouse model in studying HBV-induced liver hyperplasia and its progression to HCC.

References

1. Hoshida Y, Nijman SM, Kobayashi M, Chan JA, Brunet JP, Chiang DY, et al. Integrative transcriptome analysis reveals common molecular subclasses of human hepatocellular carcinoma. Cancer Res 2009;69: 7385-7392.
2. Azam F, Koulaouzidis A. Hepatitis B virus and hepatocarcinogenesis. Ann Hepatol 2008;7:125-129.
3. Zhang X, Zhang H, Ye L. Effects of hepatitis B virus X protein on the development of liver cancer. J Lab Clin Med 2006;147:58-66.
4. Keasler VV, Lerat H, Madden CR, Finegold MJ, McGarvey MJ, Mohammed EM, et al. Increased liver pathology in hepatitis C virus transgenic mice expressing the hepatitis B virus X protein. Virology 2006;347:466-475.
5. Lee TH, Finegold MJ, Shen RF, DeMayo JL, Woo SL, Butel JS. Hepatitis B virus transactivator X protein is not tumorigenic in transgenic mice. J Virol 1990;64:5939-5947.
6. Wu BK, Li CC, Chen HJ, Chang JL, Jeng KS, Chou CK, et al. Blocking of G1/S transition and cell death in the regenerating liver of hepatitis B virus X protein transgenic mice. Biochem Biophys Res Commun 2006;340:916-928.
7. Bock CT, Toan NL, Koeberlein B, Song LH, Chin R, Zentgraf H, et al. Subcellular mislocalization of mutant hepatitis B X proteins contributes to modulation of STAT/SOCS signaling in hepatocellular carcinoma. Intervirology 2008;51:432-443.
8. Cha MY, Kim CM, Park YM, Ryu WS. Hepatitis B virus X protein is essential for the activation of Wnt/beta-catenin signaling in hepatoma cells. HEPATOLOGY 2004;39:1683-1693.
9. Huo TI, Wang XW, Forgues M, Wu CG, Spillare EA, Giannini C, et al. Hepatitis B virus X mutants derived from human hepatocellular carcinoma retain the ability to abrogate p53-induced apoptosis. Oncogene 2001;20:3620-3628.
10. Wang XW, Forrester K, Yeh H, Feitelson MA, Gu JR, Harris CC. Hepatitis B virus X protein inhibits p53 sequence-specific DNA binding, transcriptional activity, and association with transcription factor ERCC3. Proc Natl Acad Sci U S A 1994;91:2230-2234.
11. Wang XW, Gibson MK, Vermeulen W, Yeh H, Forrester K, Sturzbecher HW, et al. Abrogation of p53-induced apoptosis by the hepatitis B virus X gene. Cancer Res 1995;55:6012-6016.
12. Grompe M, al-Dhalimy M, Finegold M, Ou CN, Burlingame T, Kennaway NG, et al. Loss of fumarylacetoacetate hydrolase is responsible for the neonatal hepatic dysfunction phenotype of lethal albino mice. Genes Dev 1993;7:2298-2307.
13. Keng VW, Villanueva A, Chiang DY, Dupuy AJ, Ryan BJ, Matise I, et al. A conditional transposon-based insertional mutagenesis screen for genes associated with mouse hepatocellular carcinoma. Nat Biotechnol 2009;27:264-274.
14. Wangensteen KJ, Wilber A, Keng VW, He Z, Matise I, Wangensteen L, et al. A facile method for somatic, lifelong manipulation of multiple genes in the mouse liver. HEPATOLOGY 2008;47:1714-1724.
15. Dickins RA, Hemann MT, Zilfou JT, Simpson DR, Ibarra I, Hannon GJ, et al. Probing tumor phenotypes using stable and regulated synthetic microRNA precursors. Nat Genet 2005;37:1289-1295.
16. Bell JB, Podetz-Pedersen KM, Aronovich EL, Belur LR, McIvor RS, Hackett PB. Preferential delivery of the Sleeping Beauty transposon system to livers of mice by hydrodynamic injection. Nat Protoc 2007;2:3153-3165.
17. Doria M, Klein N, Lucito R, Schneider RJ. The hepatitis B virus HBx protein is a dual specificity cytoplasmic activator of Ras and nuclear activator of transcription factors. EMBO J 1995;14:4747-4757.
18. Lian Z, Liu J, Li L, Li X, Clayton M, Wu MC, et al. Enhanced cell survival of Hep3B cells by the hepatitis B x antigen effector, URG11, is associated with upregulation of beta-catenin. HEPATOLOGY 2006;43:415-424.
19. Calvisi DF, Factor VM, Loi R, Thorgeirsson SS. Activation of beta-catenin during hepatocarcinogenesis in transgenic mouse models: relationship to phenotype and tumor grade. Cancer Res 2001;61:2085-2091.
20. Orejuela D, Jorquera R, Bergeron A, Finegold MJ, Tanguay RM. Hepatic stress in hereditary tyrosinemia type 1 (HT1) activates the AKT survival pathway in the fah-/- knockout mice model. J Hepatol 2008;48:308-317.